

## Regular Article

# Calcined Ni–Al Complex Hydroxide and Its Use for the Removal of Phosphate Ion from Aqueous Solution

Fumihiko Ogata,<sup>a</sup> Chiharu Ito,<sup>a</sup> Megumu Toda,<sup>b</sup> Masashi Otani,<sup>b</sup> Chalermpong Saenjum,<sup>c,d</sup> Takehiro Nakamura,<sup>a</sup> and Naohito Kawasaki<sup>\*,a,e</sup>

<sup>a</sup>Faculty of Pharmacy, Kindai University, 3-4-1 Kowakae, Higashi-Osaka, Osaka 577-8502, Japan; <sup>b</sup>Kansai Catalyst Co., Ltd., 1-3-13, Kashiwagi-cho, Sakai-ku, Sakai, Osaka 590-0837, Japan; <sup>c</sup>Faculty of Pharmacy, Chiang Mai University, Suthep Road, Muang District, Chiang Mai, 50200, Thailand; <sup>d</sup>Cluster of Excellence on Biodiversity-based Economics and Society (B.BES-CMU), Chiang Mai University, Suthep Road, Muang District, Chiang Mai, 50200, Thailand; <sup>e</sup>Antiaging Center, Kindai University, 3-4-1 Kowakae, Higashi-Osaka, Osaka 577-8502, Japan

Received March 6, 2020; Accepted March 27, 2020

Calcined Ni–Al complex hydroxide (NA12) was produced through calcination at 400°C, and its capability on phosphate ion adsorption was examined. Initially, the physicochemical characteristics including specific surface area, the number of hydroxyl groups, pore volume, scanning electron microscope images, and X-ray diffraction patterns of calcined Ni–Al complex hydroxides were evaluated. The level of phosphate ion adsorbed onto NA12 in the value of 128.5 mg/g was higher than that of other compared adsorbents. This study indicated that the level of phosphate ion adsorbed using calcined Ni–Al complex hydroxide was correlated to the properties of an adsorbent surface. Moreover, the binding energy of the NA12 surface before and after the phosphate ion adsorption was also determined, and phosphorus energy (2p and 2s) could be detected after adsorption. The results demonstrated that the NA12 surface properties were important for phosphate ion removal from the aqueous solution. Additionally, the effects of pH, temperature, and contact time on the phosphate ion adsorption were also investigated. The results confirmed a potent recovery of the phosphate ion (over 90%) when using a NaOH solution at 1000 mmol/L in this experiment. Thus, NA12 is a promising adsorbent for the phosphate ion.

**Key words** Ni–Al complex hydroxide, phosphate ion, adsorption, calcination

## INTRODUCTION

Phosphorus (P) is a necessary micro-nutrient for plant growth. Excessive use of fertilizers containing P in agriculture, and the resulting runoff of P, have led to increasing eutrophication in various water environments.<sup>1–3</sup> Nevertheless, P is one of the necessary elements for all forms of life. Therefore, it is important to remove and/or recover phosphate ions from the aqueous phase effectively.<sup>4</sup>

Adsorptive removal of the phosphate ion has been more concerned, owing to its advantages, such as low energy consumption, high efficiency, reliable, and easily operation, and the facilitation of P recycling. Recently, various adsorbents have been established in use for phosphate ion removal from aqueous solutions. Interestingly, metal (hydr)oxides have been considered useful for adsorbing phosphate ion from aquatic ecosystems, owing to their unique physicochemical properties and nontoxic characteristics.<sup>5–7</sup>

In addition, calcined metal (hydr)oxides are promising adsorbents for the removal of the phosphate ion because they possess a permanent, positive layer charge (and a high specific surface area)<sup>8,9</sup> or a unique memory effect property.<sup>10</sup> The unique memory effect property facilitates rebuilding of the original structure when placed in contact with anions in aqueous solution. This property induces an increased adsorption

capability comparable to that of non-calcined materials.

Our previous studies reported that calcined Al (hydr)oxide or calcined Ni hydroxide at 400°C<sup>11,12</sup> exhibited high adsorption capability for the phosphate ion compared with that of virgin compounds. Additionally, we evaluated the capability of Ni–Al complex hydroxide for adsorbing the phosphate ion from aqueous solutions.<sup>13</sup> However, there is no report on the capacity of calcined Ni–Al complex hydroxide for the phosphate ion adsorption in aqueous solutions. Therefore, if the phosphate ion adsorption by calcined Ni–Al complex hydroxide could be explored, the value and applicability of calcined Ni–Al complex hydroxide would considerably increase.

The objective of recent study was to explore the phosphate ion adsorption capacities using calcined Ni–Al complex hydroxide prepared at 400°C and its properties were also investigated. Moreover, the adsorption kinetics, adsorption isotherms, the effect of pH on the adsorption and desorption abilities of the phosphate ion from calcined Ni–Al complex hydroxide were evaluated.

## MATERIALS AND METHODS

**Materials** Ni–Al complex hydroxides were obtained from Kansai Catalyst Co. Ltd (Japan). Compounds with the molar ratios of Ni<sup>2+</sup> to Al<sup>3+</sup> of 0.5, 1.0, 2.0, 3.0, and 4.0 were indi-

\*To whom correspondence should be addressed. e-mail: kawasaki@phar.kindai.ac.jp

cated as NA12, NA11, NA21, NA31, and NA41, respectively (They are collectively referred to as NAs henceforth). Calcination was performed via the following method. Calcined NAs were prepared by treating NAs at 400°C for 2 h in a muffle furnace. The phosphate ions solution was prepared with potassium dihydrogen phosphate (FUJIFILM Wako Pure Chemical Co., Japan).

The evaluation of crystallinities, elemental analysis, and electron spectroscopy were performed using MiniFlex II (Rigaku, Japan), JXA-8530F (JEOL, Japan), and AXIS-NOVA (Shimadzu, Japan), respectively. The pore volumes and specific surface area were analyzed using NOVA 4200e specific surface analyzer (Yuasa Ionic, Japan). The total of hydroxyl groups was analyzed using the fluoride ion adsorption method.<sup>14)</sup>

**Amount of Phosphate Ion Adsorbed** 0.05 g of the adsorbents namely NA12, NA11, NA21, NA31, and NA41 were mixed to 50 mL of 300 mg/L phosphate ion solution. The reaction mixture was shaken at 25°C and 100 rpm for 24 h. Then, the reaction mixture was filtered using a 0.45 μm membrane filter. The obtained solution was measured by adsorption spectrophotometry (DR/890, Hach, USA). The amount of phosphate ion adsorbed was calculated using Eq. (1)

$$q = (C_0 - C_e) V/W \quad (1)$$

where  $q$  is the amount of phosphate ion adsorbed (mg/g),  $C_0$  is the initial concentration (mg/L),  $C_e$  is the equilibrium concentration (mg/L),  $V$  is the solvent volume (L), and  $W$  is the weight of the adsorbent (g).

**Effect of Contact Time, pH, and Temperature on the Adsorption of Phosphate Ion** Initially, to evaluate the effect of contact time, 0.05 g of NA12 was mixed to 50 mL of 10, 30, and 50 mg/L phosphate ion solutions. The reaction mixture was shaken at 100 rpm and 25°C for 0.5, 1, 3, 6, 20, and 24 h. Then, to evaluate the effect of pH, 0.05 g of NA12 was mixed to 50 mL of 50 mg/L phosphate ion solution in the solutions pH of 2, 4, 6, 8, and 10, respectively. The pH of the reaction mixture was adjusted by hydrochloric acid or sodium hydroxide solution, and the reaction mixture was shaken at 100 rpm and 25 °C for 24 h. Finally, to evaluate the adsorption temperature effect, 0.05 g of NA12 was mixed to 50 mL of 50 mg/L phosphate ion solution. The reaction mixture was shaken at 100 rpm for 24 h at 5, 25, and 50 °C. The level of phosphate ion adsorbed was calculated using Eq. (1).

**Effect of Coexistences on the Adsorption of Phosphate Ion onto NA12** 0.05 g of NA12 was mixed to 50 mL of a 1 or 5 mmol/L phosphate ion and chloride ion, sulfate ion, or nitrate ion binary solution system. These solutions were prepared by sodium chloride, sodium sulfate, and sodium nitrate. The reaction mixtures were shaken at 100 rpm and 25°C for 24 h. Subsequently, the reaction mixtures were filtered through a 0.45 μm membrane filter. The obtained solutions were measured by adsorption spectrophotometry DR/890 (Hach, USA) or ion chromatography (DIONEX ICS-900, Thermo Fisher Scientific Inc., Japan). The quantity of phosphate ion adsorbed was calculated using Eq. (1). Measurement condition was described in a previous study.<sup>13)</sup>

**Capability of NA12 for the Adsorption and Desorption of Phosphate Ion with Sodium Hydroxide Solution** 0.3 g of NA12 was mixed to 100 mL of 300 mg/L phosphate ion solution. The reaction mixture was shaken at 100 rpm and

25°C for 24 h. Then, the reaction mixture was filtered through a 0.45 μm membrane filter. The obtained solution was analyzed by adsorption spectrophotometry DR/890 (Hach, USA). The quantity of phosphate ion adsorbed was calculated by using Eq. (1). After adsorption, the collected adsorbent was dried, and then used for the desorption experiment. The collected NA12 was mixed to 50 mL of sodium hydroxide solution in the concentrations of 1, 10, 100, and 1000 mmol/L. Then, the reaction mixtures were shaken at 100 rpm and 25°C for 24 h and subsequently filtered through a 0.45 μm membrane filter. The concentration of the phosphate ion released from NA12 was quantified by adsorption spectrophotometry (DR/890, Hach, USA). The amount of phosphate ion desorbed was calculated using Eq. (2)

$$d = C_e V/W \quad (2)$$

where  $d$  is the amount desorbed (mg/g),  $C_e$  is the equilibrium concentration (mg/L),  $V$  is the solvent volume (L), and  $W$  is the weight of the adsorbent (g). The results in this study are presented as means±standard deviations (S.D.,  $n = 2-3$ , all experiments)

## RESULTS AND DISCUSSION

**Properties of Adsorbent** Scanning electron microscope images and X-ray diffraction (XRD) patterns of the adsorbents are illustrated in Fig. 1. The NAs contained spherical particles of numerous diameters and mainly Jamborite and Nickel oxide. Our previous study reported that untreated NAs contained mainly Nickel hydroxide.<sup>13)</sup> Therefore, we obtained different structures of NAs via calcination in this experimental condition. Hence, we evaluated the physicochemical characteristics of the NAs (Table 1). The quantity of hydroxyl groups, specific surface area, and pore volume of NA12 or NA11 were higher than those of other adsorbents. Similar trends were reported previously.<sup>13)</sup> Particularly, these properties of calcined NAs (the quantity of hydroxyl groups and specific surface area of NA12 and NA11 was 2.44±0.11 mmol/g and 77.8±1.6 m<sup>2</sup>/g, and 2.00±0.08 mmol/g and 15.1±1.8 m<sup>2</sup>/g, respectively) were higher than those of virgin ones (the amount of hydroxyl groups and specific surface area of NA12 and NA11 was 1.62 mmol/g and 26.4 m<sup>2</sup>/g, and 1.92 mmol/g and 22.8 m<sup>2</sup>/g, respectively).<sup>13)</sup>

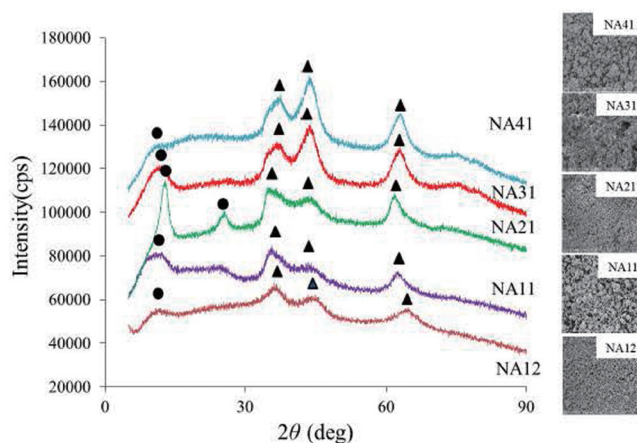
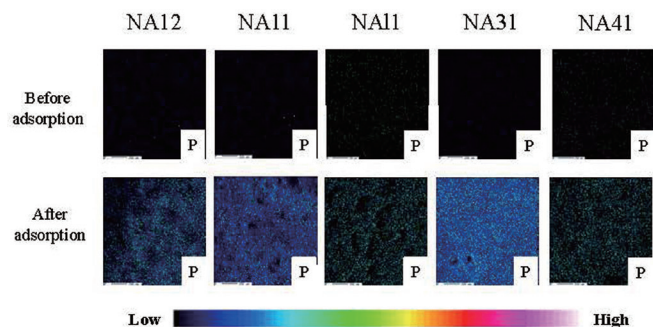


Fig. 1. SEM Images and XRD Patterns of Adsorbents

● Jamborite, Ni(OH)<sub>2</sub>(NiOOH); ▲ Nickel Oxide, NiO

**Table 1.** Physicochemical Characteristics of Adsorbents

Samples	Amount of hydroxyl groups (mmol/g)	Specific surface area (m <sup>2</sup> /g)	Pore volume (mL/g)		
			$d \leq 20\text{\AA}$ ( $\times 10^{-3}$ )	$20\text{\AA} < d \leq 500\text{\AA}$ ( $\times 10^{-2}$ )	$d > 500\text{\AA}$ ( $\times 10^{-2}$ )
NA12	2.44 ± 0.11	77.8 ± 1.6	156 ± 5	23.8 ± 0.07	5.7 ± 0.6
NA11	2.00 ± 0.08	15.1 ± 1.8	0.637 ± 8.5	8.24 ± 6.6	3.64 ± 1.1
NA21	1.07 ± 0.02	8.16 ± 3.0	0.0964 ± 0.2	6.0 ± 1.1	3.27 ± 0.2
NA31	1.13 ± 0.02	5.17 ± 5.2	0.433 ± 0.2	5.92 ± 0.04	2.81 ± 0.2
NA41	1.03 ± 0.06	8.86 ± 2.0	0.294 ± 0.07	5.46 ± 0.2	2.46 ± 0.2

**Fig. 2.** Qualitative Analysis of Adsorbents Surface Before and After Adsorption of Phosphate Ion

**Amount of Phosphate Ion Adsorbed** The amounts of phosphate ion adsorbed onto NA12, NA11, NA21, NA31, and NA41 were 128.5±15.5, 89.5±12.5, 29.0±2.0, 33.0±6.0, and 68.0±17.0 mg/g, respectively. We calculated the relationship between the amount of phosphate ion adsorbed and the physicochemical characteristics. The correlation coefficients between the amount of phosphate ion adsorbed and the quantity of hydroxyl groups, specific surface area, micropore, mesopore, and macropore structure were 0.906, 0.854, 0.804, 0.848, and 0.793, respectively. Results from the recent experiments demonstrated that the amount of phosphate ion adsorbed is related to the physicochemical characteristics of NAs. Additionally, Figure 2 revealed the adsorbent surface before and after the adsorption of the phosphate ion. The increase in P content was confirmed after adsorption treatment. The properties of the adsorbent surface are important factors for the phosphate ion removal from aqueous solutions. Moreover, the binding energy of the adsorbent (NA12) before and after adsorption was also investigated and exhibited in Fig. 3. The P(2p) and P(2s) peaks were detected after adsorption, which indicate that phosphate ions were adsorbed onto the adsorbent surface of NA12. Simultaneously, we could confirm the decrease in S(2p) peak. Our studies had been demonstrated previously that the possibility of phosphate ion adsorption mechanisms when using metal complex hydroxide was ion exchange with anions in the interlayer of the metal complex hydroxide.<sup>15)</sup> In this study, the NAs were prepared using sulfates and have a layered double hydroxide structure. Finally, we confirmed that the amount of phosphate ion adsorbed and the amount of sulfate ion released from the NA adsorbent were emphatically correlated in this experiment ( $r = 0.969$ ), confirming that sulfate ions inter-layered in the NA adsorbent are exchanged with phosphate ions.

**Effect of Contact Time on the Adsorption of Phosphate Ion** To understand the adsorption equilibrium, the effect of contact time on the phosphate ion adsorption onto NA12 is exhibited in Fig. 4. The adsorption equilibrium was established within 3 h. Previous studies reported that, when using synthe-

sized Zn-Al LDH, zirconium-loaded carbon nanotube, Mg-Al layered double hydroxide, and Fe-Mn oxide adsorbent, the adsorption equilibrium of the phosphate ion was established within 8, 5, 5, and 3.3 h, respectively. These results indicate that NA12 is functional for the phosphate ion removal from aqueous solutions.<sup>16-19)</sup>

To elucidate the adsorption rate and possibility of kinetic mechanisms, the results were analyzed using the pseudo-first-order (Eq. (3)) and pseudo-second-order (Eq. (4)) kinetic models<sup>20,21):</sup>

$$\ln(q_e - q_t)/q_e = -k_1 t \quad (3)$$

$$t/q_t = 1/(k_2 q_e^2) + t/q_e \quad (4)$$

where  $q_e$  and  $q_t$  are the amounts of phosphate ion adsorbed at equilibrium and at time  $t$  (mg/g), respectively;  $k_1$  is the pseudo-first-order rate constant ( $\text{h}^{-1}$ ); and  $k_2$  is the pseudo-second-order rate constant ( $\text{g/mg/h}$ ).

The kinetic parameters calculated are summarized in Table 2. It is clear that the fit of the pseudo-second-order model ( $r = 0.999$ ) is better than that of the pseudo-first-order model ( $r = 0.057-0.923$ ). Moreover, the calculated amount of adsorbent,  $q_{e, \text{cal}}$  (10.2±0.37, 30.4±0.13, and 51.8±0.13 mg/g for 10, 30, and 50 mg/L initial concentrations, respectively) in the pseudo-second-order model was correlate to the actual experimental amount of adsorbent used,  $q_{e, \text{exp}}$  (10.8±0.40, 31.3±1.08, and 51.9±0.01 mg/g for 10, 30, and 50 mg/L initial concentrations, respectively). Our results can suggest here that the mechanism of phosphate ion adsorption onto the NA12 surface might be chemisorption.<sup>22)</sup>

**Effect of pH on the Adsorption of Phosphate Ion** Figure 5 illustrated the effects of the pH value of the initial solution on the phosphate ion adsorption by NA12. NA12 exhibited good capacity for phosphate ion adsorption in the initial pH range from 2.0 to 12.0. Similar trends had been reported previously.<sup>23-26)</sup> The point of neutral charge of NA12 was approximately 6.0. In this study, the pH of the solution after adsorption ranged from 4.0 to 6.5; therefore, the positively charged surface favored adsorption, owing to the electrostatic interaction between the positive charge of adsorbent surface and the negative charge of phosphate ions.<sup>25)</sup> In the pH range from 3.0-7.2,  $\text{H}_2\text{PO}_4^-$  was the dominant species in the phosphate solution. The free energy of  $\text{H}_2\text{PO}_4^-$  adsorption was lower than that of  $\text{HPO}_4^{2-}$  or  $\text{PO}_4^{3-}$ , and hence,  $\text{H}_2\text{PO}_4^-$  was more efficiently adsorbed by NA12 comparable to  $\text{HPO}_4^{2-}$  or  $\text{PO}_4^{3-}$ .<sup>24,27-29)</sup>

**Effect of Temperature on the Adsorption of Phosphate Ion** The adsorption isotherms for the phosphate ion adsorption onto NA12 were investigated in three different temperatures. Figure 6 indicates that the amount of phosphate ion adsorbed elevated with the increase in adsorption temperatures, suggesting that phosphate ion adsorption onto NA12

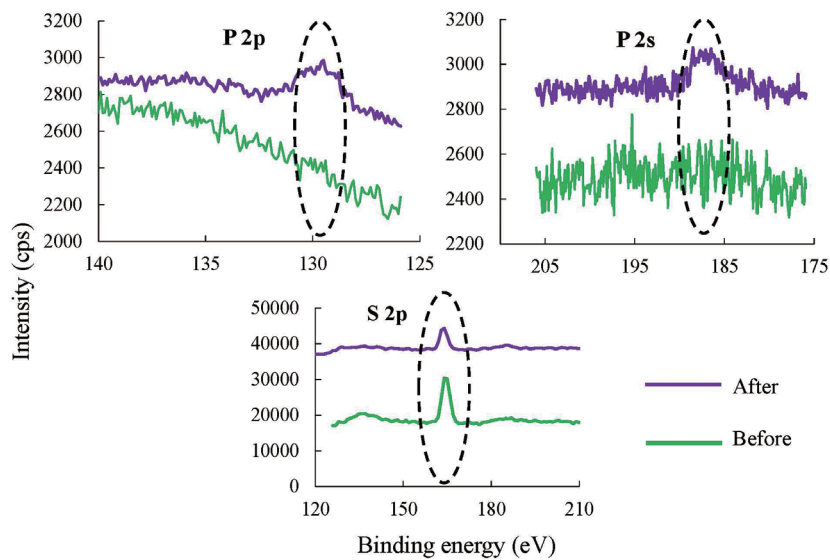


Fig. 3. Binding Energy of NA12 Surface Before and After Adsorption of Phosphate Ion

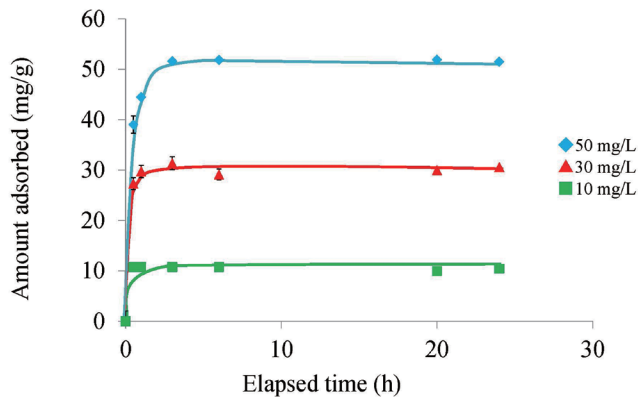


Fig. 4. Effect of Contact Time on the Adsorption of Phosphate Ion onto NA12

Initial concentration 10, 30, and 50 mg/L, solvent volume 50 mL, adsorbent 0.05 g, contact time 0.5, 1, 3, 6, 20, and 24 h, temperature 25°C, agitation speed 100 rpm

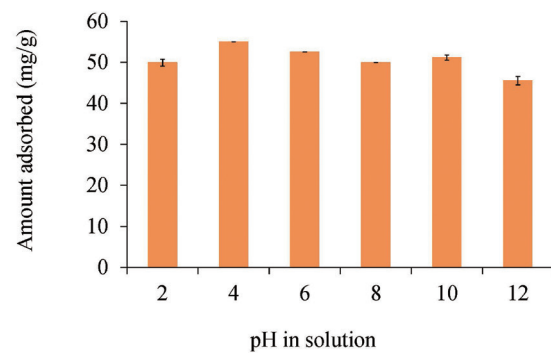


Fig. 5. Effect of pH on the Adsorption of Phosphate Ion at Different pH Conditions

Initial concentration 50 mg/L, solvent volume 50 mL, adsorbent 0.05 g, contact time 24 h, solution pH 2-12, temperature 25°C, agitation speed 100 rpm

Table 2. Kinetic Parameters for the Adsorption of Phosphate Ion

Initial concentration (mg/L)	$q_{e,exp}$ (mg/g)	Pseudo-first-order model			Pseudo-second-order model		
		$k_1$ (h <sup>-1</sup> )	$q_{e,cal}$ (mg/g)	$r$	$k_2$ (g/mg/h)	$q_{e,cal}$ (mg/g)	$r$
10	10.8 ± 0.40	0.8 ± 0.07	0.022 ± 8.01	0.699	1.0 ± 0.64	10.2 ± 0.37	0.999
30	31.3 ± 1.08	0.056 ± 0.01	3.1 ± 1.08	0.057	0.52 ± 0.04	30.4 ± 0.13	0.999
50	51.9 ± 0.01	0.97 ± 0.005	23.6 ± 0.11	0.923	0.21 ± 0.06	51.8 ± 0.13	0.999

was an endothermic mechanism.<sup>30</sup>) To confirm the mechanism of phosphate ion adsorption, the isotherm data were further fitted to two commonly used isotherm models namely Langmuir (Eq. 5) and Freundlich (Eq. 6).

$$C_e/q_e = 1/W_s a + C_e/W_s \quad (5)$$

where  $C_e$  is the equilibrium concentration (mg/L),  $q_e$  is the amount adsorbed at equilibrium (mg/g), and  $W_s$  and  $a$  are the Langmuir constants related to the monolayer adsorption capacity and the energy of sorption, respectively, and

$$\log q_e = \log k + (1/n) \log C_e \quad (6)$$

where  $k$  and  $n$  are the Freundlich constants related to the adsorption of the adsorbent and the intensity of adsorption, respectively.

Table 3 exerts the Langmuir and Freundlich constants for the phosphate ion adsorption. It can be observed that the Langmuir and Freundlich models were fitted to the data of an experiments ( $r = 0.835$ – $0.967$  and  $0.883$ – $0.989$ ). The Langmuir constant  $W_s$  raised with the increase in adsorption temperature, indicating the endothermic mechanism of the adsorption process. Moreover, phosphate ions were comfortably

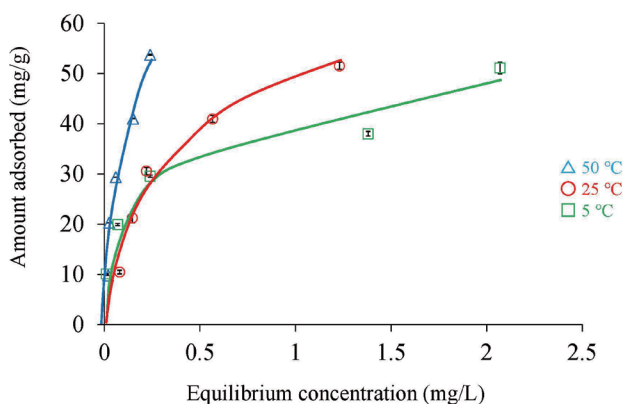


**Fig. 6.** Adsorption Isotherms of Phosphate Ion

Initial concentration 10, 20, 30, 40, and 50 mg/L, solvent volume 50 mL, adsorbent 0.05 g, contact time 24 h, temperature 5, 25, and 50°C agitation speed 100 rpm

adsorbed onto the NA12 surface when  $1/n$  was in the range of 0.1–0.5, but not when  $1/n > 2$ .<sup>31)</sup> The value of  $n^{-1}$  ( $0.4 \pm 0.08$ – $0.6 \pm 0.29$ ) suggested that the phosphate ions adsorption onto the NA12 surface occurred readily, owing to chemisorption.<sup>13)</sup> Thus, the phosphate ion adsorption onto NA12 is attributed to monolayer adsorption in this study.

Additionally, the thermodynamics of phosphate ion adsorption was also investigated. The thermodynamic parameters, i.e., standard Gibbs free energy ( $\Delta G$ ), standard enthalpy change ( $\Delta H$ ), and standard entropy change ( $\Delta S$ ), were estimated using Eqs. (7) and (8)

$$\Delta G = -RT \ln K \quad (7)$$

$$\ln K = \Delta S/R - \Delta H/RT \quad (8)$$

where  $R$  is the universal gas constant (8.314 J/mol/K),  $T$  is the absolute temperature (K), and  $K$  is the adsorption equilibrium constant. Thus,  $\Delta H$  and  $\Delta S$  are determined from the slope and intercept.

The obtained  $\Delta G$  values for 278, 298, and 323 K were -4.54, -4.62, and -5.38 kJ/mol, respectively, and the obtained  $\Delta H$  and  $\Delta S$  were 0.61 kJ/mol and 18.2 J/mol/K, respectively. The  $\Delta G$  value decreased with the increase in temperature, suggesting an increase in the spontaneity of the reaction.<sup>32)</sup> The positive value of  $\Delta H$  indicated the endothermic mechanism of the phosphate ion adsorption process, which was also indicated by the enhanced phosphate ion adsorption amounts at higher temperature.<sup>19)</sup> In addition, the positive value of  $\Delta S$  indicated an increase in disorder at the solid–solution interface during the phosphate ion adsorption process.<sup>33)</sup>

**Effect of Coexistences on the Adsorption of Phosphate Ion** The level of phosphate ion adsorbed in the complex solution system is illustrated in Fig. 7. Results of recent experiments indicates the initial concentration of 1 mmol/L, coexistence anions including chloride ion, nitrate ion, and sulfate ion did not affect the phosphate ion adsorption capability. However, the coexistence anions affected the adsorption capability at the initial concentration of 5 mmol/L. From the results, the sulfate ion (divalent ion) was more strongly affected the adsorption capability. Similar trends had been reported previously.<sup>27,34)</sup> Additionally, the phosphate ion, nitrate ion, and chloride ion formed an inner-sphere complex with the hydroxyl groups at the adsorbent surface. However, the sulfate ion

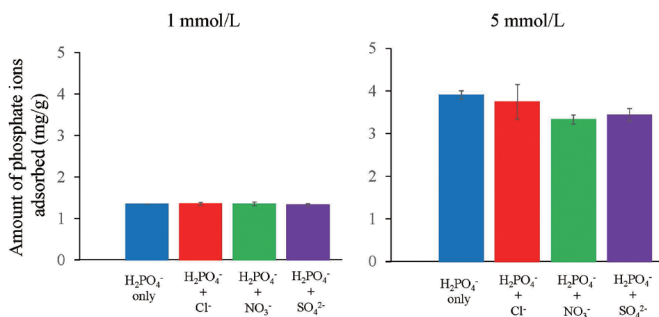


**Fig. 7.** Amount of Phosphate Ion Adsorbed in Complex Solution System

Initial concentration 1 or 5 mmol/L, adsorbent 0.05 g, contact time 24 h, temperature 25°C, agitation speed 100 rpm

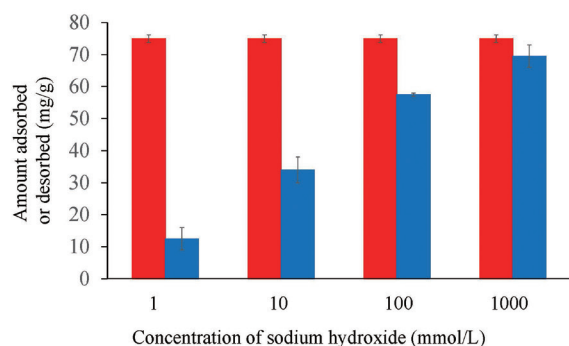


**Fig. 8.** Amount of Phosphate Ion Adsorbed or Desorbed

Adsorption condition: Initial concentration 300 mg/L, solvent volume 100 mL, adsorbent 0.3 g, contact time 24 h, temperature 25°C, agitation speed 100 rpm. Desorption condition: Initial concentration 1, 10, 100, and 1000 mmol/L, solvent volume 50 mL, adsorbent 0.3 g, contact time 24 h, temperature 25°C, agitation speed 100 rpm.

can be adsorbed by forming an outer-sphere or inner-sphere complex, and therefore, it competes with the phosphate ion better than that of nitrate ion or chloride ions. Thus, NA12 exhibited good capability for the phosphate ion adsorption in a complex solution system.

**Recovery of Phosphate Ion Using NA12** To determine the desorption ability of the phosphate ion by NA12, desorption experiments were performed under various concentrations of sodium hydroxide solution (Fig. 8). The desorption rate of the phosphate ion raised with the increase in alkalinity from 1 to 1000 mmol/L. The phosphate ion desorption rate increased from 16.7% to 92.7%, indicating that the bonding between the adsorbed phosphate ion and the active site was breakable and the phosphate adsorbed onto NA12 can be desorbed at high pH. It was proved that NA12 could be used as a reusable adsorbent.

To confirm the NA12 structure after adsorption, we investigated the XRD patterns of NA12 before and after the phosphate ion adsorption (Fig. S1). The diffraction peak (003) indicates the stacking of brucite-like sheets.<sup>35–38)</sup> The shift of this  $2\theta$  peak decreased slightly, because a part of adsorbed phosphate ion remained in NA12. Therefore, the desorption rate is not fully 100% in this experiment. Moreover, we confirmed that the NA12 structure is not destroyed after adsorption. Finally, we investigated the phosphate ion after adsorption (Fig. S2). The desorbed phosphate ion was in the form of

**Table 3.** Langmuir and Freundlich Constants for the Adsorption of Phosphate Ion

Temperature(°C)	Langmuir constants		Freundlich constants			
	<i>Ws</i> (mg/g)	<i>a</i> (L/mg)	<i>r</i>	log <i>k</i>	1/ <i>n</i>	<i>r</i>
5	37.6 ± 0.003	38.0 ± 0.29	0.964	1.6 ± 0.04	0.4 ± 0.08	0.989
25	49.3 ± 0.01	25.4 ± 0.34	0.967	1.7 ± 0.22	0.5 ± 0.04	0.887
50	96.2 ± 0.03	6.9 ± 0.04	0.835	2.1 ± 0.38	0.6 ± 0.29	0.883

sodium hydrogen phosphate or sodium dihydrogen phosphate, which indicates that the desorbed material can be reused as a fertilizer in this experiment.

In summary, we prepared calcined NA12 in this study and evaluated its capability for phosphate ion adsorption from the aqueous phase. The capability for the phosphate ion adsorption onto NA12 increased compared with that of virgin NA12, and the adsorption was related to its physicochemical properties. Particularly, ion exchanges between the phosphate ions and sulfate ions released from NA12 were highly correlated (0.969) in this experiment. In addition, the adsorption mechanisms were elucidated via binding energy or elemental analysis.

At the initial 1 mmol/L sodium hydroxide solution, coexistence anions (chloride ion, nitrate ion, and sulfate ion) did not affect the phosphate ion adsorption capability in the complex solution system. The adsorbed phosphate ion can be desorbed from NA12 using sodium hydroxide solution at different concentrations, and its form (sodium hydrogen phosphate or sodium dihydrogen phosphate) was observed using XRD patterns before and after adsorption. Thus, calcined NA12 is a potential candidate to be used for adsorption and recovery of the phosphate ion in aqueous solutions.

**Acknowledgment** This research was funded by The Research Foundation for Pharmaceutical Sciences.

**Conflict of interest** The authors declare no conflict of interest.

## REFERENCES

- Huang Y, Lee X, Grattieri M, Yuan M, Cai R, Macazo FC, Minteer SD. Modified biochar for phosphate adsorption in environmentally relevant conditions. *Chem. Eng. J.*, **380**, 122375 (2020).
- Veni DK, Kannan P, Edison TNJI, Senthilkumar, A. Biochar from green waste for phosphate removal with subsequent disposal. *Waste Manag.*, **68**, 752–759 (2017).
- Vikrant K, Kim KH, OK YS, Tsang DCW, Tsang YF, Giri BS, Singh RS. Engineered/designer biochar for the removal of phosphate in water and wastewater. *Sci. Total Environ.*, **616–617**, 1242–126 (2018).
- Bennett E, Elser J. A broken biogeochemical cycle. *Nature*, **478**, 29–3 (2011).
- He J, Xu Y, Wang W, Hu B, Wang Z, Yang X, Wang Y, Yang L. Ce(III) nanocomposites by partial thermal decomposition of Ce-NOF for effective phosphate adsorption in a wide pH range. *Chem. Eng. J.*, **379**, 122431 (2020).
- Riddle M, Cederlind H, Schmieder F, Bergström L. Magnetite-coated biochar as a soil phosphate filter: from laboratory to field lysimeter. *Geoderma*, **327**, 45–54 (2018).
- Hao H, Wang Y, Shi B. NaLa(CO<sub>3</sub>)<sub>2</sub> hybridized with Fe<sub>3</sub>O<sub>4</sub> for efficient phosphate removal: synthesis and adsorption mechanistic study. *Water Res.*, **155**, 1–11 (2019).
- Liu C, Zhang M, Pan G, Lundehøj L, Nielsen UG, Shi Y, Hansen HCB. Phosphate capture by ultrathin MgAl layered double hydroxide nanoparticles. *Appl. Clay Sci.*, **177**, 82–90 (2019).
- Hibino T, Jones W. New approach to the delamination of layered double hydroxides. *J. Mater. Chem.*, **11**, 1321–1323 (2001).
- Seftel EM, Ciocarlan RG, Michielsen B, Meynen V, Mullens S, Cool P. Insights into phosphate adsorption behavior on structurally modified ZnAl layered double hydroxides. *Appl. Clay Sci.*, **165**, 234–246 (2018).
- Kawasaki N, Ogata F, Takahashi K, Kabayama M, Kakehi K, Tanada S. Relationship between anion adsorption and physicochemical properties of aluminum oxide. *J. Health Sci.*, **54**, 324–329 (2008).
- Ogata F, Imai D, Toda M, Otani M, Kawasak N. Properties of a novel adsorbent produced by calcination of nickel hydroxide and its capability for phosphate ion adsorption. *J. Ind. Eng. Chem.*, **34**, 172–179 (2016).
- Ogata F, Toda M, Otani M, Nakamura T, Kawasaki N. Evaluation of phosphate ion adsorption from aqueous solution by nickel-aluminum complex hydroxides. *Water Sci. Technol.*, **2017**, 913–921 (2018).
- Ymashita T, Ozawa Y, Nakajima N, Murata T. Ion exchange properties and uranium adsorption of hydrous titanium (IV) oxide. *Nippon Kagaku Kaishi*, **8**, 1057–1061 (1978).
- Yang K, Yan LG, Yang YM, Yu SJ, Shan RR, Yu HQ, Zhu BC, Du B. Adsorptive removal of phosphate by Mg-Al and Zn-Al layered double hydroxides: kinetics, isotherms and mechanisms. *Separ. Purif. Tech.*, **124**, 36–42 (2014).
- Hatami H, Fotovat A, Halajnia A. Comparison of adsorption and desorption of phosphate on synthesized Zn-Al LDH by two methods in a simulated soil solution. *Appl. Clay Sci.*, **152**, 333–341 (2018).
- Yifan G, Mengmeng Y, Weili W, Runping H. Phosphate adsorption from solution by zirconium-loaded carbon nanotubes in Batch mode. *J. Chem. Eng. Data*, **64**, 2849–2858 (2019).
- Luengo CV, Volpe MA, Avena MJ. High sorption of phosphate on Mg-Al layered double hydroxides: kinetics and equilibrium. *J. Environ. Chem. Eng.*, **5**, 4656–4662 (2017).
- Xiaoli D, Qiang H, Junqi L, Haiyan L. The behavior of phosphate adsorption and its reactions on the surfaces of Fe-Mn oxide adsorbent. *J. Taiwan Inst. Chem. Eng.*, **76**, 167–175 (2017).
- Ho YS, McKay G. The kinetics of sorption of divalent metal ions onto sphagnum moss peat. *Water Res.*, **34**, 735–742 (2000).
- Langergren S. Zur theorie der sogenannten adsorption geloster stoffe. *K. Sven. Vetenskapsakad. Handl.*, **24**, 1–39 (1898).
- Ho YS. Review of second-order models for adsorption systems. *J. Hazard. Mater.*, **136**, 681–689 (2006).
- Ogata F, Nagai N, Kishida M, Nakamura T, Kawasaki N. Interaction between phosphate ions and Fe-Mg type hydroxide for purification of wastewater. *J. Environ. Chem. Eng.*, **7**, 102897 (2019).
- Jiang D, Amano Y, Machida M. Removal and recovery of phosphate from water by a magnetic Fe<sub>3</sub>O<sub>4</sub>@ASC adsorbent. *J. Environ. Chem. Eng.*, **5**, 4229–4238 (2017).
- Deng L, Shi Z. Synthesis and characterization of a novel Mg–Al hydroxide-loaded kaolin clay and its adsorption properties for phosphate in aqueous solution. *J. All. Comp.*, **637**, 188–196 (2015).
- Kong L, Tian Y, Li N, Liu Y, Zhang J, Zhang J, Zuo W. Highly-effective phosphate removal from aqueous solutions by calcined nanoporous palygorskite matrix with embedded lanthanum hydroxide. *Appl. Clay Sci.*, **162**, 507–517 (2018).
- Liao XP, Ding Y, Wang B, Shi B. Adsorption behavior of phosphate on metal-ions-loaded collagen fiber. *Ind. Eng. Chem. Res.*, **45**, 3896–3901 (2006).
- Chubar N, Kanibolotskyy V, Strelko V, Gallios G, Samanidou V, Shaposhnikova T, Milgrandt V, Zhuravlev I. Adsorption of phosphate ions on novel inorganic ion exchangers. *Colloids Surf. A Physicochem. Eng. Asp.*, **255**, 55–63 (2005).
- Chowdhury SR, Yanful EK. Arsenic and chromium removal by mixed magnetite–maghemite nanoparticles and the effect of phosphate on

- removal. *J. Environ. Manage.*, **91**, 2238–2247 (2010).
- 30) Mezenner NY, Bensmaili A. Kinetics and thermodynamic study of phosphate adsorption on iron hydroxide-eggshell waste. *Chem. Eng. J.*, **147**, 87–96 (2009).
- 31) Abe I, Hayashi M, Kitagawa M. Studies on the adsorption of surfactants on activated carbon. *J. Jap. Oil Chem. Soc.*, **25**, 145–150 (1976).
- 32) Liu T, Wu K, Zeng L. Removal of phosphorus by a composite metal oxide adsorbent derived from manganese ore tailings. *J. Hazard. Mater.*, **217-218**, 29–35 (2012).
- 33) Yan LG, Xu YY, Yu HQ, Xin XD, Wei Q, Du B. Adsorption of phosphate from aqueous solution by hydroxy-aluminum, hydroxyl-iron and hydroxyl-iron-aluminum pillared bentonites. *J. Hazard. Mater.*, **179**, 244–250 (2010).
- 34) Wang J, Tong X, Wang S. Zirconium-modified activated sludge as a low-cost adsorbent for phosphate removal in aqueous solution. *Water Air Soil Pollut.*, **229**, 47 (2018).
- 35) Ogata F, Kawasaki N. Adsorption of As(III) from aqueous solutions by novel Fe-Mg type hydrotalcite. *Chem. Pharm. Bull. (Tokyo)*, **63**, 1040–1046 (2015).
- 36) Ogata F, Ueta E, Kawasaki N. Characteristics of a novel adsorbent Fe-Mg-type hydrotalcite and its adsorption capability of As(III) and Cr(VI) from aqueous solution. *J. Ind. Eng. Chem.*, **59**, 56–63 (2018).
- 37) Türk T, Alp İ. Arsenic removal from aqueous solutions with Fe-hydrotalcite supported magnetite nanoparticle. *J. Ind. Eng. Chem.*, **20**, 732–738 (2014).
- 38) Ookubo A, Ooi K, Hayashi H. Phase transition of Cl-intercalated hydrotalcite-like compound during ion exchange with phosphates. *Langmuir*, **10**, 407–411 (1994).